Crystal/Glass Phase Change in KSb_5S_8 Studied through Thermal Analysis Techniques

K. Chrissafis,[‡] Theodora Kyratsi,[†,‡] K. M. Paraskevopoulos,[‡] and Mercouri G. Kanatzidis*[,†]

Department of Chemistry, Michigan State University, East Lansing, Michigan 48824, and Department of Physics, Aristotle University of Thessaloniki, 54124 Thessaloniki, Greece

Received October 24, 2003. Revised Manuscript Received February 25, 2004

The reversible crystal−glass and glass−crystal transitions discovered in KSb_5S_8 were studied in detail with nonisothermal scanning calorimetry techniques. When cooled, molten KSb_5S_8 becomes a metastable glass, which can quantitatively revert to the crystalline form if heated above 277 °C. Crystalline KSb_5S_8 is a red semiconductor with a band gap of 1.82 eV, whereas the glass (also red) shows a lower but equally well-defined band gap of 1.67 eV. Two approaches have been used to analyze the glass transition. The activation energy of crystallization E_c was calculated using the Kissinger (∼167 ± 3.1 kJ/mol) and Flynn−Wall−Ozawa methods. The kinetic parameters and energy band gaps determined for KSb_5S_8 suggest possible utility of this system for phase-change, high-density optical data storage applications.

Introduction

Reports of reversible phase changes such as crystal−glass−crystal transformations in a single compound are relatively rare. If sufficiently rapid, a phase change can be the basis for data storage applications. The primary system used currently in such applications is thin films of $Ge_2Sb_2Te_5$ that exhibit glass to crystal transition on the nanosecond time scale.[1] In addition, materials that exhibit this property can act as rewritable storage media for polarized holograms,[2] opto-mechanical actuators,[3] nonvolatile memory,[4] and infrared optical waveguides.[5] In past reports, we have already described several stoichiometric systems that form glasses upon slow cooling from the melt including $(Ph_4P)InSe_{12}$,[6] $KSbP_2Se_6$,[7] and $Cs_2Hg_3Ge_2S_8$.[8] The glassy forms exothermically crystallize upon heating shortly after the glass transition temperature T_g is reached. Recently, we reported the phase change properties of KSb_5S_8[9] and pointed out its potential for information storage applications.[10] The observation that crystallization proceeds nearly immediately after passing through T_g indicates that the amorphous material is in a high energy state with a low barrier to crystallization. Although the class of chalcogenide glasses is very large, most have continuous, nonstoichiometric compositions, and are made entirely of covalently bonded atoms (e.g., $Ge_{1-x}Se_x$,[11] Ge−As−Se,[12] and $(Ag_2S)_x(GeS_2)_y$,[13] etc). In contrast, glassy KSb_5S_8 stands out, because, in addition to being stoichiometric, it features two types of bonding in its structure, covalent bonding in the anionic $[Sb_5S_8]^-$ framework, and ionic bonding associated with K- - -S interactions. We surmise that this mixed bonding character plays a role in the exceptionally clean and fast phase-change behavior it exhibits.

Kinetic phase-change studies in stoichiometric compounds are rare in the literature, yet such studies may yield mechanistic insight into such processes. Here we have studied in detail the glass transition and crystallization kinetics of KSb_5S_8, using differential scanning calorimetry (DSC). We also discuss the crystallization rate and activation energies with respect to those of $Ge_2Sb_2Te_5$[1] as well as possible utility in optical data storage systems.

* To whom correspondence should be addressed. E-mail: Kanatzid@cem.msu.edu.

† Michigan State University.

‡ Aristotle University of Thessaloniki.

(1) (a) Yamada, N.; Ohno, E.; Nishiuchi, K.; Akahira, N.; Takao, M. *J. Appl. Phys.* **1991**, *69*, 2849−2856. (b) Rubin, K. A.; Birnie, D. P.; Chen, M. *J. Appl. Phys.* **1992**, *71*, 3680−3687. (c) Ohta, T. *J. Optoelectron. Adv. Mater.* **2001**, *3* (3), 609−626. (d) Yamada, N.; Matsunaga, T. *J. Appl. Phys.* **2000**, *88* (12), 7020−7028.

(2) (a) Mateev, V.; Petkova, T.; Markovsky, P.; Mitkova, M. *Thin Solid Films* **1993**, *226*, 119. (b) Mitkova, M.; Petkova, T.; Markovski, P.; Mateev, V. *J. Non-Cryst. Solids* **1993**, *164−166*, 1203. (c) Ozols, A.; Nordman, N.; Nordman, O.; Riihola, P. *Phys. Rev. B* **1997**, *55*, 14236. (d) Spektor, B.; Lisiansky, M.; Shamir, J.; Klebanov, M.; Lyubin, V. *Appl. Phys. Lett.* **2000**, *76*, 798.

(3) (a) Tikhomirov, V. K.; Elliott, S. R. *Phys. Rev.* **1994**, *B49*, 17476. (b) Fritzsche, H. *Semiconductors* **1998**, *32*, 850.

(4) Nakayama, K.; Kojima, K.; Imai, Y.; Kasai, T.; Fukushima, S.; Kitagawa, A.; Kumeda, M.; Kakimoto, Y.; Suzuki, M. *Jpn. J. Appl. Phys. Part 1* **2003**, *42*, 404.

(5) (a) Balan, V.; Vigreux, C.; Pradel, A.; Ribes, M. *J. Optoelectron. Adv. Mater.* **2001**, *3* (2), 367. (b) Lucas, J. *Curr. Opin. Solid State Mater. Sci.* **1999**, *4* (2), 181−187. (c) Saito, M.; Kikuchi, K. *Opt. Rev.* **1997**, *4*, 527.

(6) Dhingra, S.; Kanatzidis, M. G. *Science* **1993**, *258*, 1769.

(7) Breshears, J. D.; Kanatzidis, M. G. *J. Am. Chem. Soc.* **2000**, *122*, 7839.

(8) Marking, G. A.; Hanko, J. A.; Kanatzidis, M. G. *Chem. Mater.* **1998**, *10*, 1191.

(9) (a) Berlepsch, P.; Miletich, R.; Armbruster, Th. *Z. Kristallogr.* **1999**, *214*, 57. (b) Berlepsch, P.; Miletich, R. *Schweiz. Miner. Petrogr. Mitt.* **1997**, *78*, 185.

(10) Chrissafis, K.; Kyratsi, T.; Wachter, J.; Paraskevopoulos, K. M.; Kanatzidis, M. G. *Adv. Mater.* **2003**, *15*, 1428.

(11) Wang, Y.; Boolchand, P.; Micoulaut, M. *Europhys. Lett.* **2000**, *52*, 633.

(12) Balan, V.; Vigreux, C.; Pradel, A.; Ribes, M. *J. Optoelectron. Adv. Mater.* **2001**, *3*, 367.

(13) Etienne, S.; Perez, J.; Peytavin, S.; Ribes, M. *J. Solid State Chem.* **1991**, *92*, 27.

10.1021/cm035065q CCC: $27.50
Published on Web 04/16/2004

Experimental Section

Synthesis. KSb_5S_8 was formed as a crystalline ingot by reacting a stoichiometric combination of potassium metal, antimony, and sulfur. A mixture of 0.130 g of K (3.32 mmol), 2.0193 g of Sb (16.59 mmol), and 0.8510 g of S (26.54 mmol) was loaded into a silica tube and sealed under vacuum (10^{-4} Torr). The mixture was heated at 850 °C for 1 h and cooled to room temperature at a rate of ~15 °C/h. KSb_5S_8 was obtained as dark red platelike crystals in quantitative yield. Glassy KSb_5S_8 was obtained after remelting the crystals (melt must be kept under inert atmosphere or vacuum) and quenching the melt in water or air.[14]

Thermal Analysis. The differential scanning calorimetric (DSC) measurements were carried out with a Setaram DSC141 calorimeter. Temperature and energy calibrations of the instrument were performed, for different heating rates, using the well-known melting temperatures and melting enthalpies of high-purity zinc and indium supplied with the instrument. Bulk-shaped specimens weighing about 7 mg were crimped in aluminum crucibles; an empty aluminum crucible was used as reference. A constant flow of nitrogen was maintained to provide a constant thermal blanket within the DSC cell, thus eliminating thermal gradients and ensuring the validity of the applied calibration standard from sample to sample. DSC runs were made at five different heating rates, i.e., 10, 15, 20, 25, and 30 K/min. The temperature range covered in DSC was from room temperature through their T_g to 650 K.

Theoretical Basis of Solid-State Kinetic Analysis. Kinetic analysis of solid-state transformations is usually based on a single-step kinetic equation

$$d\alpha/dt = k(T)f(\alpha) \tag{1}$$

where $k(T)$ is the rate constant, t is the time, T is the temperature, α is the fractional extent of reaction, and $f(\alpha)$ is the reaction model. The explicit temperature dependence of the rate constant is introduced by replacing $k(T)$ with the Arrhenius equation, which gives

$$d\alpha/dt = A \exp(-E/RT)f(\alpha) \tag{2}$$

where A (the preexponential factor) and E (the activation energy) are the Arrhenius parameters and R is the gas constant. For nonisothermal conditions, $d\alpha/dt$ in eq 2 is replaced with $\beta(d\alpha/dT)$, where $\beta(=dT/dt)$ is the heating rate. The ratio of the kinetic process $d\alpha/dt$ is proportional to the measured specific heat flow ϕ, normalized per sample mass (W/g):

$$d\alpha/dt = \phi/\Delta H_c \tag{3}$$

where ΔH_c corresponds to the total enthalpy change associated with the crystallization process. The fractional extent of reaction α can be easily obtained by partial integration of nonisothermal thermal analysis curve.

The crystallization kinetics is usually interpreted in terms of the standard nucleation-growth model formulated by Johnson−Mehl−Avrami (JMA).[15,16] This model describes the time dependence of the fractional extent of reaction α, usually written in the following form:

$$\alpha = 1 - \exp[-(kt)^n] \tag{4}$$

where the rate constant k is a function of temperature and in general depends on both the nucleation frequency and the crystal growth rate, and the kinetic exponent n is a parameter which reflects the nucleation frequency and/or the growth morphology.[16] The rate equation can be obtained from eq 4 by differentiation with respect to time:

$$(d\alpha/dt) = kn(1 - \alpha)[-\ln(1 - \alpha)]^{1-1/n} \tag{5}$$

Equation 5 is usually referred to as the JMA equation, and it is frequently used for the formal description of thermal crystallization data. It should be emphasized, however, that the validity of the JMA equation is based on the following assumptions: (a) isothermal crystallization conditions, (b) low anisotropy of growing crystals, (c) homogeneous nucleation or heterogeneous nucleation at randomly dispersed second-phase particles, and (d) growth rate of new phase controlled by temperature and independent of time.

Henderson[17,18] has shown that the validity of the JMA equation can be extended in nonisothermal conditions if the entire nucleation process takes place during the early stages of the transformation and it becomes negligible afterward. The crystallization rate is controlled only by temperature and does not depend on the previous thermal history. Although the limits of applicability of the JMA equation are well-known, in practice it is not so easy to verify whether or not the conditions of applicability are fulfilled. Several methods have been proposed to test the applicability of the JMA model and we examined our nonisothermal data by two of them.

The most popular testing method for nonisothermal data is an inspection of the linearity of the Avrami (JMA) plot. Matusita et al.,[19] extending the use of the JMA equation, have suggested an equation which is applicable for nonisothermal crystallization and is given by

$$\ln[-\ln(1 - \alpha)] = -n \ln(\beta) - 1.052\, mE_c/RT + \text{const.} \tag{6}$$

where α is the volume of the fraction crystallized at any temperature and m and n are numerical factors depending on the nucleation process and growth morphology. Here, n is equal to $(m + 1)$ for a quenched glass containing no nuclei and n is equal to m[20] for a glass containing a sufficiently large number of nuclei. Also, $m = 3$ for three-dimensional growth of crystal particles, $m = 2$ for two-dimensional growth, and $m = 1$ for one-dimensional growth. The plot of $\ln[-\ln(1 - \alpha)]$ as a function of reciprocal temperature $1/T$ should be linear. Nevertheless, it is well-known that a double logarithmic function, in general, is not very sensitive to subtle changes to its argument. Therefore, one can expect to observe substantial linearity in the plots of $\ln[-\ln(1 - \alpha)]$ versus $1/T$ even in the case that the JMA model is not fulfilled.

Another test for the applicability of the JMA model is based on the properties of the $y(\alpha)$ and $z(\alpha)$ functions (see below). Taking into account eqs 1−3, the kinetic equation for the JMA model can be written as

$$\phi = \Delta H_c\, A \exp(-E/RT)f(\alpha) \tag{7}$$

where the function $f(\alpha)$ is an algebraic expression of the JMA model

$$f(\alpha) = n(1 - \alpha)[-\ln(1 - \alpha)]^{1-1/n} \tag{8}$$

The $f(\alpha)$ function should be invariant with respect to procedure parameters such as sample mass and heating rate for nonisothermal conditions. Malek has shown[21,22] that the functions $\phi(t)$ and $\phi(T)$ are proportional to the $y(\alpha)$ and $z(\alpha)$ functions that can easily be obtained by a simple transformation of DSC data. In nonisothermal conditions these functions are defined as follows:

(14) In addition to KSb_5S_8, a new phase on this system was found with formula close to $K_3Sb_{8.66}S_{13}$. Its structure is monoclinic, $P2_1/m$ space group, with cell parameters a = 9.2407(8) Å, b = 28.173(2) Å, c = 9.2563(8) Å, β = 96.1950(10)°, V = 2375.7(4) Å^3. Kyratsi, T.; Kanatzidis, M. G., work in progress.

(15) Avrami, M. *J. Chem. Phys.* **1941**, *9*, 177.

(16) Johnson, W. A.; Mehl, R. F. *Trans. Am. Inst. Min.* (*Metall.*) *Eng.* **1939**, *135*, 416.

(17) Henderson, D. W. *J. Therm. Anal.* **1979**, *15*, 325.

(18) Henderson, D. W. *J. Non-Cryst. Solids* **1979**, *30*, 301.

(19) Matusita, K.; Konatsu, T.; Yokota, R. *J. Mater. Sci.* **1984**, *19*, 291.

(20) Matusita, K.; Sakka, S. *Phys. Chem. Glasses* **1979**, *20*, 81.

(21) Malek, J. *Thermochim. Acta* **1989**, *138*, 337.

(22) Malek, J. *Thermochim. Acta* **1995**, *267*, 61.

$$y(\alpha) = \phi \exp(E_c/RT) \quad (9)$$

$$z(\alpha) = \phi T^2 \quad (10)$$

For practical reasons the $y(\alpha)$ and $z(\alpha)$ functions are normalized within the 0−1 range. The maxima exhibited by the $y(\alpha)$ and $z(\alpha)$ functions are defined as α_M and α_p^{∞} respectively. The maximum of the $z(\alpha)$ function α_p^{∞} is a constant for the JMA model ($\alpha_p^{\infty} = 0.632$) and a characteristic "fingerprint" for it.[22]

Results and Discussion

The crystal structure of KSb_5S_8 presents an infinitely extended anionic framework of distorted SbS_6 octahedra. The Sb−S network has a strong two-dimensional character.[10] The K ions are found in cavities of this framework and there exist ionic K- - -S interactions. Crystals of KSb_5S_8 melt at 441 °C but cooling the liquid does not crystallize the material, it leads instead to a glassy state. X-ray diffraction shows the sample to be amorphous, containing only trace amounts of crystalline phase. In a second cycle, a strong and sharp exothermic peak is observed at 287 °C during heating of the glass, which is attributed to a glass→crystal transformation. Therefore, glassy KSb_5S_8 is metastable and can quantitatively revert back to the crystalline form.

Activation Energy of the Glass Transition, T_g. The lack of byproducts formed during the process provides an excellent opportunity to study the glass transition and crystallization kinetics of this material in detail using quantitative measurements performed with the DSC technique.

A typical DSC curve for a sample of KSb_5S_8 obtained at heating rate β of 20 K/min is shown in Figure 1. Two characteristic events are evident in the DSC thermogram. The first corresponds to the glass transition (endothermic reaction) and the second to the crystallization (exothermic reaction). Three characteristic temperatures are given in the thermogram: the glass transition (T_g = 222.7 °C), produced by the intersection of the curve and the halfway line between the two baselines, the onset temperature of crystallization (T_o = 281.0 °C), and the peak temperature of crystallization (T_p = 287.3 °C). As can be seen in Table 1, T_g increases with increasing heating rate, as would be expected. Theoretically, T_g is defined as the temperature at which the relaxation time τ becomes equal to the experimental time of observation τ_{obs}. At the same time, T_g varies inversely[23] with relaxation time. With increasing heating rate, τ_{obs} decreases and hence the glass transition temperature increases.

The dependence of T_g on the heating rate can be studied through the relation[24]

$$T_g = A + B \log \beta \quad (11)$$

where A and B are constants for a given glass composition. The value of B is related to the method of sample preparation (the lower the cooling rate the lower the B value) and its physical significance seems to be the response of the configurational changes within the glass transition region to the heating rate. A plot of T_g vs log β for the as-prepared samples is shown in Figure 2. The value of B (9.60 ± 0.56) was obtained from the figure using least-squares fit with correlation factor >0.99. The value of A (483.5 ± 0.7 K) gives the exact $T_{g-real} = A$ value by extrapolation of the data to $\beta = 1$, as the T_g vs log β function is linear.[25]

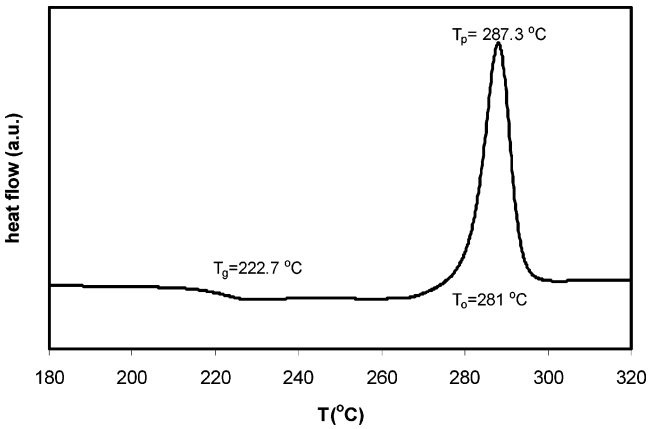

Figure 1. Typical DSC trace of KSb_5S_8 at a heating rate of 20 K/min.

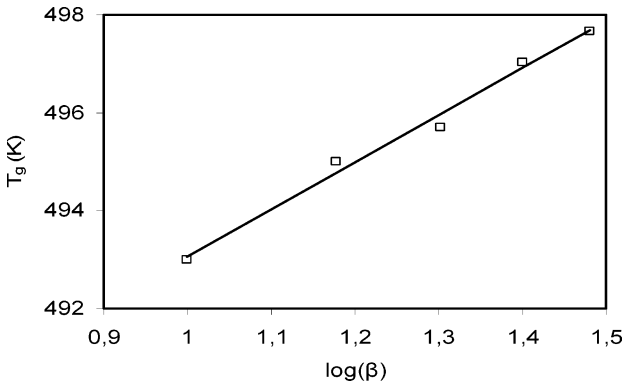

Figure 2. Plot of T_g vs log β for the as-prepared sample.

Table 1. Characteristic Temperatures and Enthalpies of the Crystallization Process of KSb_5S_8

rate (°C/min)	T_g (°C)	T_p (°C)	α_p	ΔH (kJ/mol)	m
10	220.0	277.6	0.59	68.8	6.4
15	222.0	283.4	0.58	71.7	5.7
20	222.7	287.3	0.60	73.1	4.8
25	224.0	291.1	0.57	74.9	4.8
30	224.7	293.9	0.60	78.1	4.2

To determine the activation energy of glass transition (E_g) we considered the Kissinger formula,[26] which is most commonly used in analyzing crystallization data in DSC. This formula that holds in very general cases, is suggested to be valid for glass transitions and has the form

$$\ln(\beta/T_g^2) = -E_g/RT_g + \text{const.} \quad (12)$$

where R is the universal gas constant. The value of E_g is obtained from the slope of $\ln(\beta/T_g^2)$ vs $1/T_g$ plot as is the common practice, although there is some controversy whether accurate values of E_g can be obtained

(23) Joshi, S. R.; Pratar, A.; Saxena, N. S.; Saksena, M. P. *J. Mater. Sci. Lett.* **1994**, *13*, 77.

(24) Lasocka, M. *Mater. Sci. Eng.* **1976**, *23*, 173.

(25) The value of real glass formation temperature. T_{g-real}, is necessary for the calculation of the true values of glass formation ability and the thermal stability of glasses.

(26) Colmenero, J.; Barandiaran, J. M. *J. Non-Cryst. Solids* **1978**, *88*, 263.

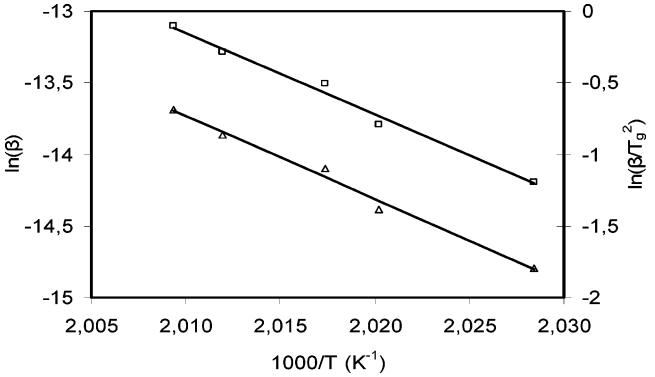

Figure 3. (a) Plot of ln (β/T_g^2) vs 1000/T_g (triangles) and (b) plot of ln β vs 1000/T_g (β in K s^{-1}) of the studied glass (squares).

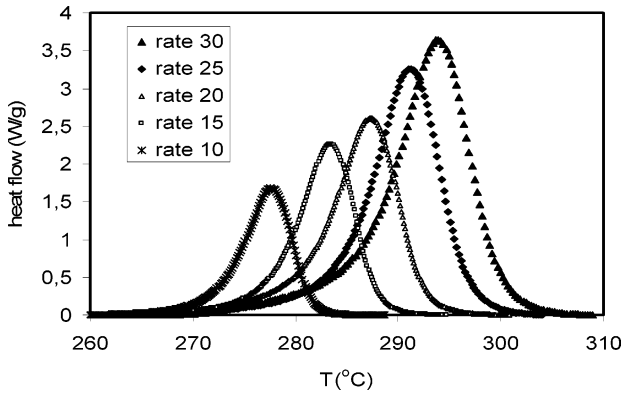

Figure 4. Nonisothermal DSC crystallization curves under different heating rates.

from the heating rate dependence of T_g for glasses formed at a constant cooling rate.[27] In addition, with the usually valid assumption that the change in ln T_g^2 with β is negligibly small[28] compared to the change in ln β, eq 12 can be written as

$$\ln \beta = -E_g/RT_g + \text{const.} \qquad (13)$$

from which the value of E_g can be obtained from the slope of a straight line of a ln β vs $1/T_g$ plot.

In Figure 3 we present the plots of ln(β/T_g^2) (curve a) and ln β (curve b) vs $1/T_g$, which display the linearity of the equations used. The values of the activation energy obtained for the glass transition are 476.0 ± 28.3 kJ/mol (plot a) and 484.3 ± 28.3 kJ/mol (plot b), respectively. These are rather large activation barriers compared to many nonstoichiometric chalcogen-rich glasses and may be a consequence of the rigid, highly connected, and continuous nature of the $[Sb_5S_8]^-$ framework, as well as the absence of "floppy" regions[29] in the structure.

Glass to Crystal Conversion: Kinetics and Activation Energy. The exothermic crystallization peaks (corrected for baseline) for all different heating rates are presented in Figure 4. It is clear that the peak temperature, T_p, shifts higher with increasing heating rate, while at the same time the peak height increases. The area under the crystallization exotherm, in the heat flow

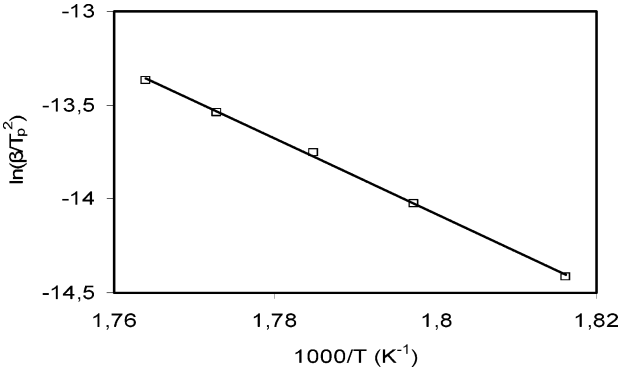

Figure 5. Experimental plot of ln(β/T_p^2) vs 1000/T_p and the corresponding straight regression line of KSb_5S_8 (β in K s^{-1}).

versus time diagram, remains constant (data not shown). This behavior can be understood if we accept that the crystallization of an amorphous state consists of two individual processes: nucleation and growth. For glasses to nucleate, a certain period of incubation is necessary. As the heating rate increases, the time available for a desired temperature to be reached is reduced and thus crystallization lags and initiates at relatively higher temperatures, i.e., the T_p correspondingly shifts to higher temperature. Generally, glasses undergo structural relaxation through which they transform from a metastable to a stable state during crystallization. The time for this transformation is shortened with increasing heating rate, preventing the entire energy of structure relaxation from being released. This part of unreleased energy is contained in the crystallization enthalpy, which is determined by the area of the DSC exotherm. The peak temperature, T_p, the volume fraction transformed, α_p at T_p, and $-\Delta H$ are also listed in Table 1.

The activation energy of crystallization (E_c) was estimated using both the Kissinger's [30] and Ozawa, Flynn, and Wall (OFW)[31] methods. Kissinger's method relates the dependence of T_p on β (heating rate) by the following equation

$$\ln(\beta/T_p^2) = -E_c/RT_p + \ln(A^*R/E_c) \qquad (14)$$

The value of E_c (167 ± 3.1 kJ/mol) was obtained from the slope of ln(β/T_p^2) vs $1/T_p$ plot given in Figure 5 and also the preexponential factor A (7.76×10^{13} s^{-1}), from the intercept. The value of the rate constant for the peak temperature is 2.1×10^{-2} s^{-1} determined for heating rate 20 K/min. By comparison, the rate constant for the peak temperature in $Ge_2Sb_2Te_5$ is 2.45×10^{-2} s^{-1} as it is calculated from the data given therein, for the same heating rate.[32]

The isoconversional method of Ozawa, Flynn, and Wall (OFW) is in fact a "model free" method which involves measuring the temperatures corresponding to fixed values of α from experiments at different heating rates β. Plotting ln(β) against $1/T$ according to eq 15

$$\ln(\beta) = \ln[Af(\alpha)/(d\alpha/dT)] - E_c/RT \qquad (15)$$

should give straight lines, the slopes of which are

(27) Hodge, I. M. *J. Non-Cryst. Solids* **1994**, *169*, 211.
(28) Sestak, J. *Phys. Chem. Glasses* **1974**, *15*, 137.
(29) Chubynsky, M. V.; Thorpe, M. F. *Curr. Opin. Solid State Mater.* **2001**, *5*, 525.
(30) Kissinger, H. E. *J. Res. Natl. Bur. Stand.* **1956**, *57*, 217.
(31) Ozawa, T. *J. Thermal Anal.* **1970**, *2*, 301.
(32) Park, J.; Kim, M.; Choi, W.; Seo, H.; Yeon, C. *Jpn. J. Appl. Phys.* **1999**, *38*, 4775.

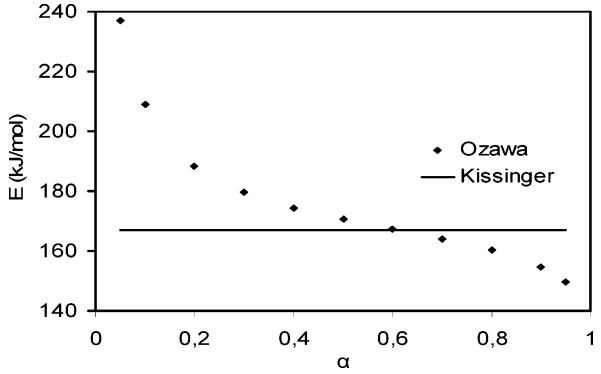

Figure 6. Activation energy E_c as a function of fractional extent of reaction α calculated from DSC data with the OFW method for the crystallization of KSb_5S_8.

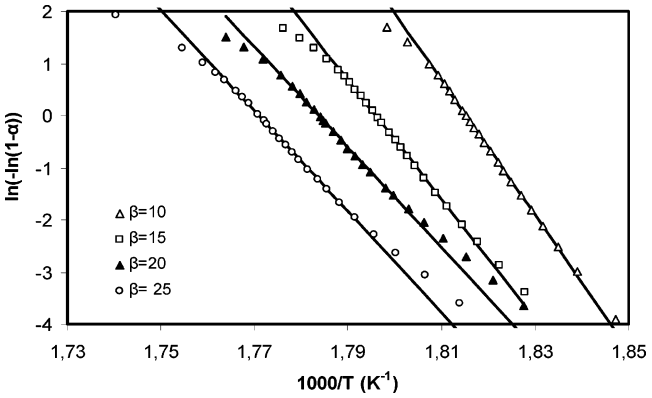

Figure 7. Plot of $\ln[-\ln(1 - \alpha)]$ against $1/T$ at different heating rates.

directly proportional to the activation energy ($-E_c/R$). If the determined activation energy is the same for the various values of α_i, the existence of a single-step reaction can be concluded with certainty. In contrast, a change of E_c with increasing degree of conversion is an indication of a complex reaction mechanism that invalidates the separation of variables involved in the OFW analysis.[33] These complications are especially serious if the total reaction involves competitive reaction mechanisms. Figure 6 shows the dependence of activation energy E_c with the fractional extent of reaction α, and it is clear that it varies substantially with α, so the results should be interpreted in terms of multistep mechanisms.

To test further the above indication, we examined the applicability of the JMA model to the experimental data by the aforementioned methods, assuming a single-step crystallization process. Figure 7 shows the Avrami plots of $\ln[-\ln(1 - \alpha)]$ against $1/T$ at different heating rates. The plots are linear over a wide temperature range, for $\alpha = 0.1-0.9$, and thus to a first approximation, the experimental data can be studied with the nucleation-growth model of Avrami according to eq 5. From the slope of the lines in the plot of Figure 7 we can calculate the coefficient m values using eq 6, taking into account the value of the activation energy E_c (167 ± 3.1 kJ/mol) derived from the application of the Kissinger model. The values of kinetic exponent m for each of the experimental heating rates, given in Table 1, were obtained from the plot using least-squares fitting with a correlation

(33) Ozawa, T. *Bull. Chem. Soc. Jpn.* **1965**, *38*, 1881.

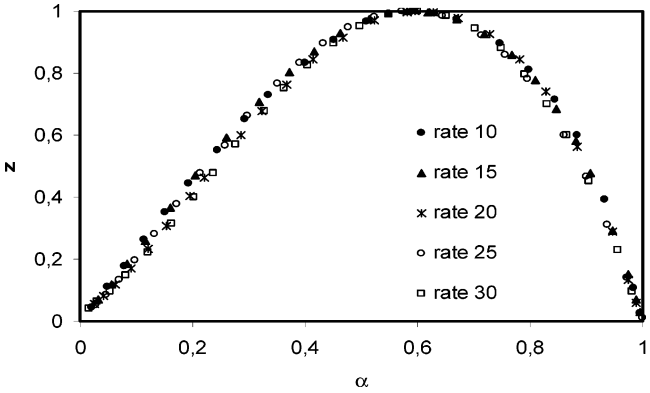

Figure 8. Normalized $z(\alpha)$ function obtained by transformation of DSC data (for different heating rates) for the crystallization of KSb_5S_8.

factor >0.999. The values of m, ranging from 4.2 to 6.4, are higher than those theoretically predicted from the JMA model and appear to decrease with increasing heating rate. These can be attributed to either the nonvalidity of the single-step reaction assumption, or perhaps the nonapplicability of Avrami plots for the experimental data, although the linear behavior in the plot, for the range of $0.1 < \alpha < 0.9$, is quite good. The experimental values (4.2−6.4) for the exponent m (determined by the nucleation mode and by the dimensionality of the crystal growth) indicate that the system undergoes bulk crystallization and that its nucleation rate increases with time. Similar values for m are received when the JMA model is used for best fitting the experimental data of Figure 4, in the form of α versus T.

Given the uncertainty regarding the applicability of the Avrami method that arises from the above discussion, we used the second mentioned test method introduced by Malek[21,22] and calculated the peak position of the $z(\alpha)$ function for the different heating rates. As can be seen in Figure 8 the peak position of the $z(\alpha)$ function, for the different heating rates, stays constant with heating rate ($\alpha \approx 0.57-0.6$). These values are slightly lower than the acceptable range of values (0.61−0.65), and we can conclude that the conditions of validity of the JMA model are not fully satisfied. This deviation indicates increasing complexity of the process, and probably, to a certain degree, mutual overlapping of the nucleation and growth phases. In fact, different nucleation and growth mechanisms may simultaneously occur in the crystallization process, thus making impossible the description of $f(\alpha)$ by means of a single JMA-type function.[34]

Phase-Change Implications for Optical Storage Applications. Generally, the important materials characteristics for phase-change optical memory applications are as follows: (a) the presence of an optical absorption edge that shifts in energy concurrent with the phase transition; (b) a suitable melting point that allows the materials to be melted with the available laser power but not too low for self-crystallization to occur (depending on the configuration, this condition may be met with melting points over a wide range, e.g., 300−1000 °C); and (c) a rapid and stable phase-transition process.

(34) Cebollada, F.; Gonzalez, J. M.; Julian, C.; Surinach, S. *Phys. Rev. B* **1997**, *56*, 6056.

In the case of KSb_5S_8 we have a substantial shift from 1.82 eV or 681 nm in the crystalline form to 1.67 eV or 743 nm in the glass. Furthermore, the melting point and the glass transition temperature are about half of the melting temperature. In this work we have shown that KSb_5S_8 exhibits crystallization kinetics similar to $Ge_2Sb_2Te_5$. It would be interesting to estimate in thin films of KSb_5S_8 the crystallization speed and the cyclability of reversible phase transitions between the amorphous and crystalline states. For good cyclability the material needs to have no large compositional deviations during phase change. Glass−crystal transitions that produce phase separation are not optimal for phase-change optical storage applications. In KSb_5S_8 we have constant stoichiometric compositions.

In KSb_5S_8 there is a large energy difference between the two states and also a suitable activation energy. Its value as extracted from DSC measurements is ∼167 kJ/mol, while the value for $GeSb_4Te_7$ (the fastest) is ∼146.7 kJ/mol, for $GeSb_2Te_4$ is ∼175.6 kJ/mol, and for $Ge_2Sb_2Te_5$ is 215.2 kJ/mol.[35]

Both the crystalline and glassy forms are dark red, but the crystalline form has a band gap of 1.82 eV while the glass shows a lower optical threshold at 1.67 eV. The small but significant narrowing of the optical band gap in the glass phase is attributed to "band tailing" effects in the extrema of the conduction and valence bands.[9] These tailing effects could arise from defects created by the rapid cooling process that resulted in the glass phase.

Conclusions

KSb_5S_8 is a congruently melting, stoichiometric system that undergoes reversible crystal→glass→crystal transformation. Two approaches have been used to analyze the glass transition. The activation energy of crystallization E_c was calculated to be ∼167 ± 3.1 kJ/mol using the Kissinger and Flynn−Wall−Ozawa equations. The results obtained with the isoconversional method of FWO for the E_c−α dependence and tests regarding the applicability conditions of the JMA model for our nonisothermal DSC data, suggest that the glass-to-crystal conversion in KSb_5S_8 is a process of increasing mechanistic complexity with time. It involves several simultaneous different nucleation and growth events. Intuitively, this is a surprising result given the apparent chemical simplicity of the crystallization process, underscoring the challenges associated with attempting to delineate solid-state mechanisms. The kinetic parameters and energy band gaps determined for KSb_5S_8 suggest possible utility of this system for phase-change, high-density optical data storage applications using lasers with considerably shorter wavelengths than those currently employed, or perhaps even using other mechanisms to effect the phase change (e.g., electrical pulses).

The high crystallization speeds of KSb_5S_8 may be attributed to the average degree of covalency in the Sb−S bonds of the framework and to the presence of the nondirectional ionic K- - -S interactions. In $Ge_2Sb_2Te_5$ all the bonds in the structure are covalent and its high crystallization speed is attributed to the relatively weak nature of the Ge−Te and Sb−Te bonds. The presence of ionic bonds in the structure may facilitate atomic motion during the transition. Therefore, very high crystallization speeds may be anticipated in alkali metal containing ternary (such as KSb_5S_8) and perhaps even quaternary chalcogenide systems.

In future work we will address the structure of the glassy state with the aid of pair distribution functions,[36] spectroscopic studies of the glass to crystal conversion, and thermal analysis studes of other alkali metal derivatives such as $TlSb_3S_5$, $RbSb_5S_8$, and solid solutions of the type $K_{1-x}Rb_xSb_5S_8$.[37] The latter studies will help assess the role of the ionicity of the alkali−S bonds on the crystallization rates.

Acknowledgment. This material is based upon work supported by the National Science Foundation under Grant DMR-0127644.

CM035065Q

(35) (a) Yamada, N. *MRS Bull.* **1996**, *21*, 48. (b) Yamada, N.; Ohno, E.; Nishiuchi, K.; Akahira, N.; Takao, M. *J. Appl. Phys.* **1991**, *69*, 2849.

(36) (a) Petkov, V.; Billinge, S. J. L.; Heising, J.; Kanatzidis, M. G. *J. Am. Chem. Soc.* **2000**, *122*, 11572. (b) Petkov, V.; Billinge, S. J. L.; Larson, P.; Mahanti, S. D.; Vogt, T.; Rangan, K. K.; Kanatzidis, M. G. *Phys. Rev. B* **2002**, *65*, 092105. (c) Petkov, V.; Trikalitis, P. N.; Bozin, E. S.; Billinge, S. J. L.; Vogt, T.; Kanatzidis, M. G. *J. Am. Chem. Soc.* **2002**, *121*, 10157.

(37) Wachter, J.; Malliakas, C.; Eckert, H.; Petkov, V.; Billinge, S. J. L.; Kanatzidis, M. G., work in progress.